

# Realistic and Fast 3D Atmospheric Simulations with Clouds using the GPU-accelerated SMART-G Radiative Transfer code for the 3MI instrument

Mustapha Moulana<sup>1, a)</sup>, Didier Ramon<sup>1</sup>, Céline Cornet<sup>2</sup>, Jérôme Riedi<sup>2</sup>, Mathieu Compiègne<sup>1</sup>, François Thieuleux<sup>2</sup>, Guillaume Penide<sup>2</sup>

<sup>1</sup>Hygeos, Euratechnologies, 165 Avenue de Bretagne, 59000 Lille, France.

<sup>2</sup>Université Lille, CNRS, UMR 8518 – LOA – Laboratoire d'optique atmosphérique, F-59000, France

<sup>a)</sup>mm@hygeos.com

## Introduction

With the 3MI (Multi-viewing, Multi-channel, Multi-polarization Imager) instrument, the demand for a fast and accurate 3D polarized radiative transfer code is more critical than ever. In the VNIR range, the instrument covers a field of view of 2200 km with a nadir resolution of 4 km<sup>2</sup> (509×509-pixel camera), and with 14 acquisitions (14 viewing directions) for the same target [1]. To meet these requirements, we use SMART-G [2], a GPU-parallelized polarized radiative transfer code. We have validated its proper consideration of the 3D atmosphere i.e., 3D variability of clouds, molecules, and aerosols, by comparing it with IPRT reference results [3]. We then get a first quantification of the computational performance of a GPU-accelerated code (here SMART-G) compared to a reference CPU-based code (here 3DMCPOL [4]). Finally, we developed a realistic backward camera mode specifically adapted to the 3MI instrument and compared it with more conventional and less realistic simulation approaches.

## Validation

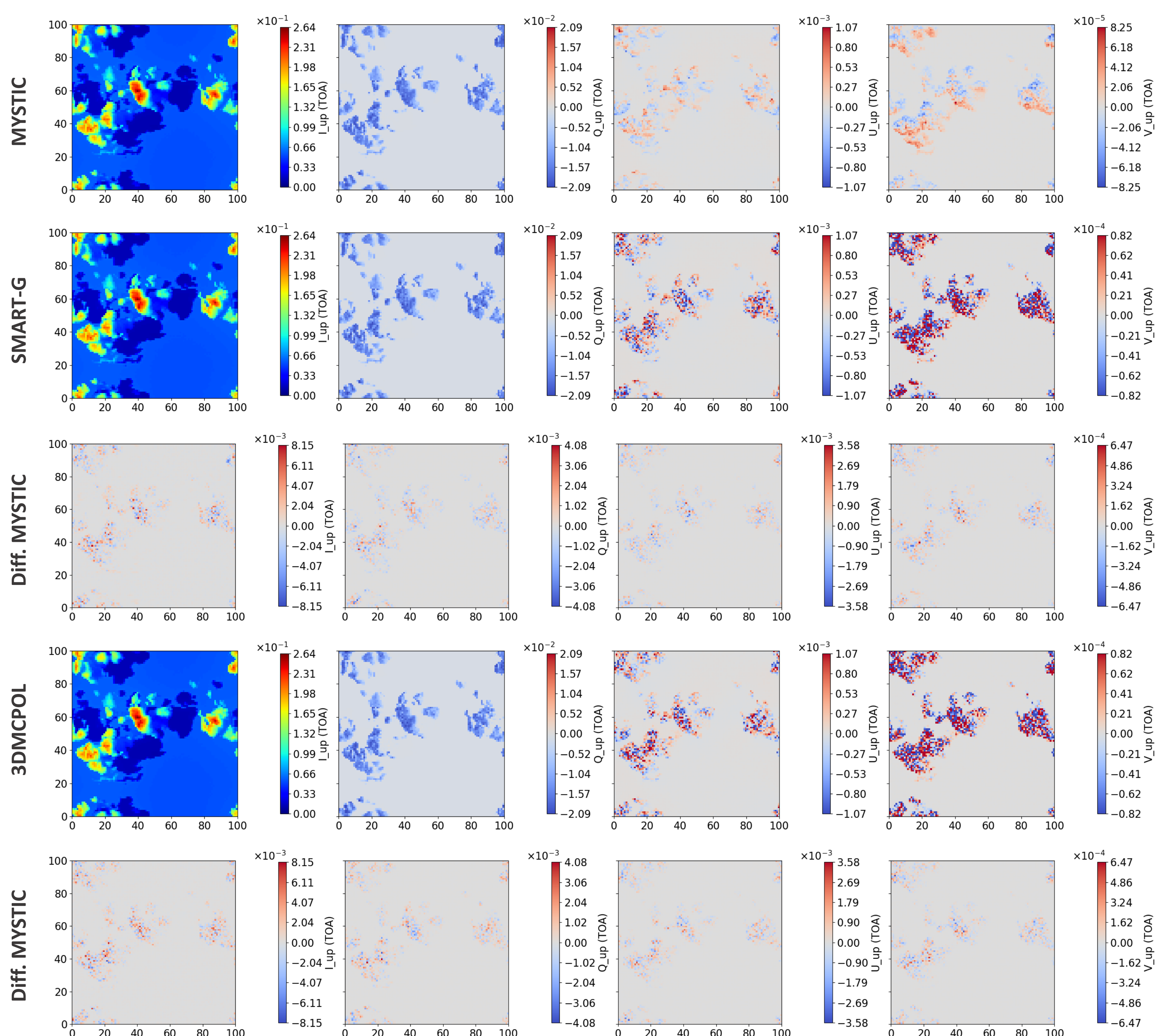
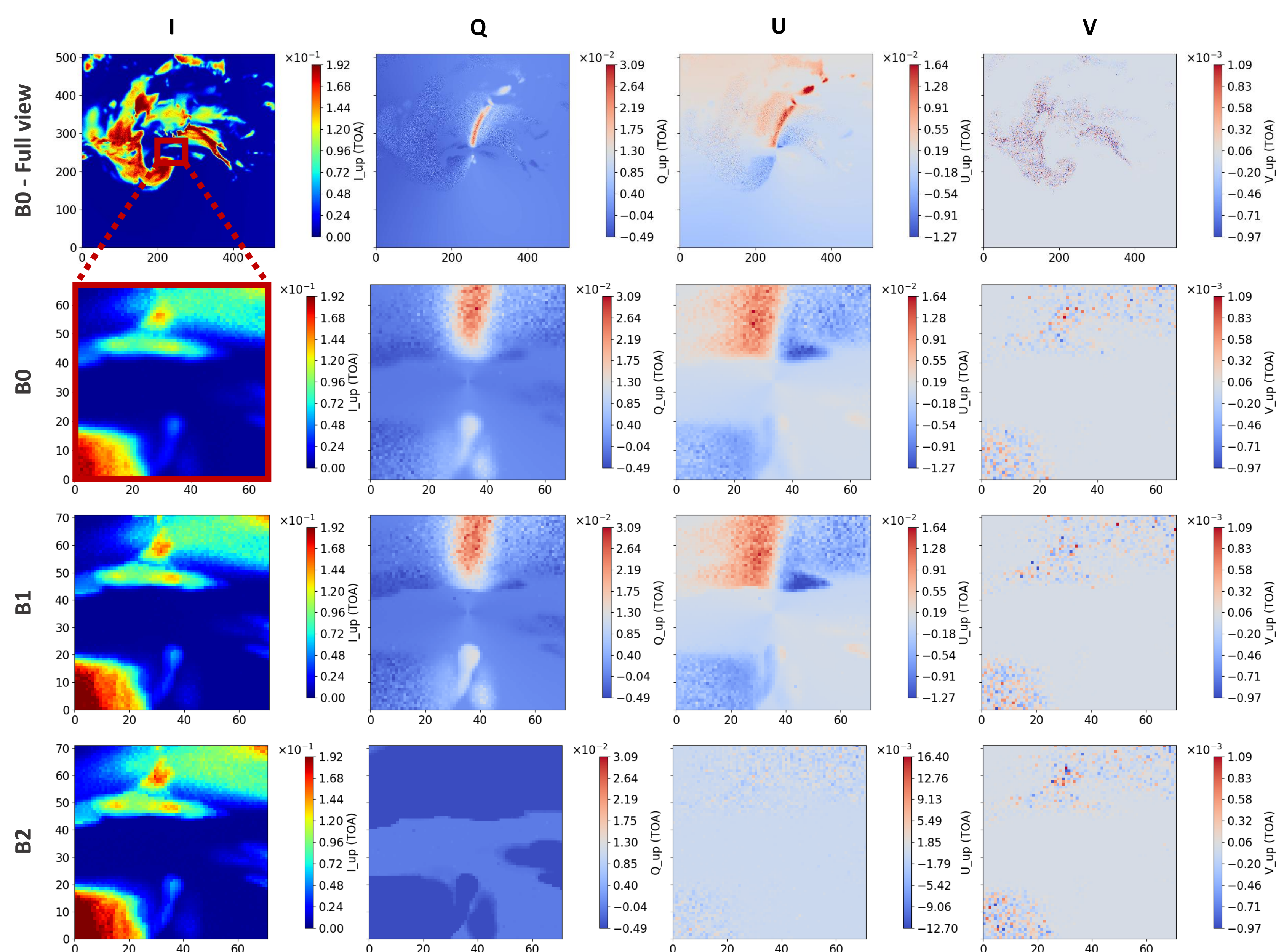


**Figure 1:** Results from MYSTIC, SMART-G and 3DMCPOL, along with the differences between SMART-G and MYSTIC, and 3DMCPOL and MYSTIC, for IPRT testcase 5 cumulus cloud in a purely molecular atmosphere.

- The validation were performed for the 2 SMART-G modes: forward and backward.

## Application to 3MI



## Perspectives

- Implementation of a cloud-specific variance reduction method such as Iwabuchi et al. [6]
- Consideration of the variability of the sun zenith and azimuth angles since we have a swath of 2200 km
- Evaluation of biases introduced by other approximate models (e.g. semi-3D with multiple 1D simulations)

- To validate the 3D atmosphere with SMART-G, we used the IPRT cases [3]. This is a comparison study with several 3D atmospheric radiative transfer codes. Comparisons are realized with the 3DMCPOL model, which participated to the intercomparison and gives results close to the reference one, which is here the MYSTIC code [5].
- All the IPRT cubic cloud (with and without the molecular atmosphere) and cumulus cloud (purely molecular and with aerosols), totalling 4x9 testcases, were validated with the same level of precision as 3DMCPOL. Figure 1 presents the results for the cumulus cloud in a purely molecular atmosphere, with the illumination conditions of the testcase 5 i.e., TOA upgoing signals with a sun zenith angle of 40° while looking at nadir.

## Benchmark

- Benchmark comparison was conducted between SMART-G (GPU-accelerated) and 3DMCPOL (CPU-accelerated).
- The same IPRT simulations used for validation were employed, except for the cumulus cloud which include aerosol.
- Hardware costs (GPU/CPU) were considered in addition to the computational time
- We observed that the GPU can be more than **20 times** cheaper than CPU for the same performance

**Table 1:** Computational time and  $\Delta m$  score [3] with MYSTIC as reference (a score close to 0 means we are closer to the reference) of simulation results from 3DMCPOL (in green) and SMART-G (in blue) of the cumulus cloud 9 testcases of without aerosol.

Model		Case 1	Case 2	Case 3	Case 4	Case 5	Case 6	Case 7	Case 8	Case 9	Total time for the 9 cases
Xeon Gold 6226R CPU 2020 7019€	I	1.38	1.37	1.13	0.87	1.08	1.23	1.33	1.33	1.31	
	Q	10.29	15.03	28.75	33.53	5.79	238.01	8	36.25	9.11	
	U	209.76	15.41	14.21	105.14	230.15	347.13	7.09	10.77	307.78	
	V	568.4	518.64	421.55	484.45	522.97	1057.02	481.23	718.89	872.1	
<b>3DMCPOL</b>	Time	1j3h44min				7j8h38min				8j12h22min	
RTX 3090 GPU 2020 4292€	I	1.41	1.38	1.15	0.90	1.09	1.20	1.29	1.41	1.39	
	Q	10.70	15.13	30.70	34.42	6.01	245.34	8.08	37.75	9.40	
	U	218.81	16.73	14.71	111.94	247.90	339.70	7.40	10.71	316.32	
	V	611.79	534.80	424.92	483.24	485.35	1014.34	509.71	707.27	895.35	
<b>SMART-G</b>	Time	6h3min37sec				1j4h8min41sec				1j10h12min	
RTX 4090 GPU 2022 4292 €	I	1.45	1.43	1.17	0.94	1.08	1.20	1.25	1.41	1.39	
	Q	10.85	15.07	30.83	35	5.79	243.15	8.25	35.67	9.25	
	U	209.49	15.79	14.41	110.09	231.96	338	7.16	10.54	325.31	
	V	572.62	539.07	417.58	484.46	499.36	1046.17	500.12	737.41	908.64	
<b>SMART-G</b>	Time	2h6min8sec				11h2min20sec				13h8min28sec	

- The atmospheric and illumination conditions are the same as the IPRT cumulus cloud testcase 5, except here we have a pure Rayleigh atmosphere from 0 to 15.7 km (TOA), with a “Medicane” cloud. The Medicane cloud simulation, using the RAMS model, was conducted on a 2200 x 2200 x 15.7 km grid, with a horizontal resolution of 4km and a vertical resolution of 0.2 km. We assumed that all the Medicane cloud is liquid for the phase matrix, with an effective radius ranging from 5 to 25 micrometers. And we used 1e6 photons per pixel.
- Three backward simulations were performed B0, B1 and B2:
  - B0** -> The more realistic. The simulation start at satellite altitude (830 km). The camera pixel is sampled i.e., pixel center direction with a FOV calculated such that the nadir pixel cover a surface of 4 km<sup>2</sup>.
  - B1** -> Starts at TOA (15,7 km). For each pixel at TOA, the direction from the pixel center to the satellite sensor is pre-calculated. Then a position inside the pixel is sampled using the pre-calculated central direction.
  - B2** -> Less realistic, same as B1 but only 1 direction (zenith) for all the pixels. Equivalent to the forward mode used for IPRT simulations.
- Those three simulations (B0 to B2) show the important impact of directional assumptions on the outgoing signals at TOA.

## References

- Lang, R., et al., 2019. The 3MI Level-1C geoprojected product—definition and processing description. *J. Quant. Spectrosc. Radiat. Transf.*, 225, 91-109.
- Ramon, D., et al., 2019. Modeling polarized radiative transfer in the ocean-atmosphere system with the GPU-accelerated SMART-G Monte Carlo code. *J. Quant. Spectrosc. Radiat. Transf.*, 222, 89-107.
- Emde, C., et al., 2018. IPRT polarized radiative transfer model intercomparison project—Three-dimensional test cases (phase B). *J. Quant. Spectrosc. Radiat. Transf.*, 209, 19-44.
- Cornet, C., et al., 2010. Three-dimensional polarized Monte Carlo atmospheric radiative transfer model (3DMCPOL): 3D effects on polarized visible reflectances of a cirrus cloud. *J. Quant. Spectrosc. Radiat. Transf.*, 111(1), 174-186.
- Mayer, B., 2009. Radiative transfer in the cloudy atmosphere. In *EPJ web of Conferences* (Vol. 1, pp. 75-99). EDP Sciences.
- Iwabuchi, H., et al., 2009. Fast and accurate radiance calculations using truncation approximation for anisotropic scattering phase functions. *J. Quant. Spectrosc. Radiat. Transf.*, 110(17), 1926-1939.